Inorg. Chem. **2007**, *46*, 7312–7320

Tetranuclear Complexes of $[Fe(CO)_2(C_5H_5)]^+$ with TCNX Ligands (TCNX = TCNE, TCNQ, TCNB): Intramolecular Electron Transfer Alternatives in Compounds $(\mu_4\text{-TCNX})[ML_n]_4$

Amarendra N. Maity,[†] Brigitte Schwederski,[†] Biprajit Sarkar,[†] Stanislav Záliš,[‡] Jan Fiedler,[‡] Sanjib Kar,[§] Goutam K. Lahiri,[§] Carole Duboc,[||] Matthias Grunert,[⊥] Philipp Gütlich,[⊥] and Wolfgang Kaim*[,†]

Institut für Anorganische Chemie, Universität Stuttgart, Pfaffenwaldring 55, D-70550 Stuttgart, Germany, J. Heyrovský Institute of Physical Chemistry, Academy of Sciences of the Czech Republic, Dolejškova 3, CZ-18223 Prague, Czech Republic, Department of Chemistry, Indian Institute of Technology, Bombay, Powai, Mumbai 400076, India, Grenoble High Magnetic Field Laboratory, MPI-CNRS, 25 Avenue des Martyrs, BP 166, F-38042 Grenoble Cedex 9, France, and Institut für Anorganische Chemie und Analytische Chemie, Johannes Gutenberg-Universität, Staudingerweg 9, D-55099 Mainz, Germany

Received November 27, 2006

The complexes $\{(\mu_4\text{-TCNX})[Fe(CO)_2(C_5H_5)]_4\}(BF_4)_4$ were prepared as light-sensitive materials from $[Fe(CO)_2(C_5H_5)(THF)](BF_4)$ and the corresponding TCNX ligands (TCNE = tetracyanoethene, TCNQ = 7,7,8,8-tetracyano-*p*-quinodimethane, TCNB = 1,2,4,5-tetracyanobenzene). Whereas the TCNE and TCNQ complexes are extremely easily reduced species with reduction potentials >+0.3 V vs ferrocenium/ferrocene, the tetranuclear complex of TCNB exhibits a significantly more negative reduction potential at about −1.0 V. Even for the complexes with strongly π-accepting TCNE and TCNQ, the very positive reduction potentials, the unusually high nitrile stretching frequencies >2235 cm^{-1}, and the high-energy charge-transfer transitions indicate negligible metal-to-ligand electron transfer in the ground state, corresponding to a largely unperturbed $(TCNX^{\circ})(Fe^{II})_4$ formulation of oxidation states as caused by orthogonality between the metal-centered HOMO and the π^* LUMO of TCNX. Mössbauer spectroscopy confirms the low-spin iron(II) state, and DFT calculations suggest coplanar TCNE and TCNQ bridging ligands in the complex tetracations. One-electron reduction to the 3+ forms of the TCNE and TCNQ complexes produces EPR spectra which confirm the predominant ligand character of the then singly occupied MO through isotropic *g* values slightly below 2, in addition to a negligible *g* anisotropy of frozen solutions at frequencies up to 285 GHz and also through an unusually well-resolved solution X band EPR spectrum of $\{(\mu_4\text{-TCNE})[Fe(CO)_2(C_5H_5)]_4\}^{3+}$ which shows the presence of four equivalent $[Fe(CO)_2(C_5H_5)]^+$ moieties through ^{57}Fe and $^{13}C(CO)$ hyperfine coupling in nonenriched material. DFT calculations reproduce the experimental EPR data. A survey of discrete TCNE and TCNQ complexes $[(\mu_4\text{-TCNX})(ML_n)_4]$ exhibits a dichotomy between the systems $\{(\mu_4\text{-TCNX})[Fe(CO)_2(C_5H_5)]_4\}^{4+}$ and $\{(\mu_4\text{-TCNQ})[Re(CO)_3(bpy)]_4\}^{4+}$ with their negligible metal-to-ligand electron transfer and several other compounds of TCNE or TCNQ with Mn, Ru, Os, or Cu complex fragments which display evidence for a strong such interaction, i.e., an appreciable value δ in the formulation $\{(\mu_4\text{-TCNX}^{\delta-})[M^{X+\delta/4}L_n]_4\}$. Irreversibility of the first reduction of $\{(\mu_4\text{-TCNB})[Fe(CO)_2(C_5H_5)]_4\}(BF_4)_4$ precluded spectroelectrochemical studies; however, the high-energy CN stretching frequencies and charge transfer absorptions of that TCNB analogue also confirm the exceptional position of the complexes $\{(\mu_4\text{-TCNX})[Fe(CO)_2(C_5H_5)]_4\}(BF_4)_4$.

Introduction

The ability of TCNE, TCNQ, and TCNB to bridge up to four metal centers and to exist in the neutral π acceptor form, as stable monoanionic radicals, or as dianions has generated a unique coordination chemistry[1] which has found potential applications in molecular magnetism,[2,3] in organic conductor research,[4] and in concepts for molecular computing.[5] Whereas

* To whom correspondence should be addressed. E-mail: kaim@iac.uni-stuttgart.de.
[†] Universität Stuttgart.
[‡] Academy of Sciences of the Czech Republic.
[§] IIT.
[||] GHMFL, MPI-CNRS.
[⊥] Johannes Gutenberg-Universität.

(1) (a) Kaim, W.; Moscherosch, M. *Coord. Chem. Rev.* **1994**, *129*, 157. (b) Miller, J. S. *Angew. Chem.* **2006**, *118*, 2570; *Angew. Chem., Int. Ed.* **2006**, *45*, 2508. (c) Bagnato, J. D.; Shum, W. W.; Strohmeier, M.; Grant, D. M.; Arif, A. M.; Miller, J. S. *Angew. Chem.* **2006**, *118*, 5448; *Angew. Chem., Int. Ed.* **2006**, *45*, 5322.

10.1021/ic062253k CCC: $37.00
Published on Web 08/11/2007

only mono- and dinuclear discrete compounds could be obtained with organometallic complex fragments of Ti,[6] V,[7] Cr,[8] and Co,[7] we have been able to establish the full coordinative saturation in tetranuclear complexes of manganese (TCNE, TCNQ),[8,9] rhenium (TCNQ),[10] ruthenium (TCNE, TCNQ, TCNB),[11] osmium (TCNE, TCNQ, TCNB),[12] and copper (TCNE, TCNQ, TCNB).[13] Except for $\{(\mu_4\text{-TCNQ})[Re(CO)_3(bpy)]_4\}^{4+}$, all these compounds showed strong evidence from spectroscopy and electrochemistry for considerable electron transfer in the ground state, an interpretation which is supported by DFT calculations for $\{(\mu_4\text{-TCNX})[Ru(NH_3)_5]_4\}^{8+}$ (TCNX = TCNE, TCNQ).[11c]

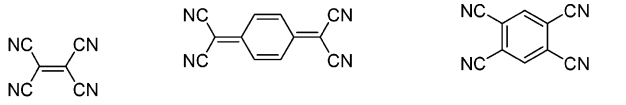

tetracyanoethene (TCNE) | 7,7,8,8-tetracyano-p-quinodimethane (TCNQ) | 1,2,4,5-tetracyanobenzene (TCNB)

In addition to the discrete tetranuclear complexes mentioned above, several coordination polymers were reported with μ_4-TCNQ[14a−e] or μ_4-TCNE[14f] of which some exhibit structural evidence for intramolecular metal-to-ligand electron transfer.

For iron there has been one report by Diaz and Arancibia describing the complex $\{(\mu_4\text{-TCNQ})[Fe(dppe)(C_5H_5)]_4\}^{4+}$, dppe = 1,2-bis(diphenylphosphino)ethane,[15a] characterized again as involving a sizable metal-to-ligand electron transfer in the ground state. Very recently, magnetic ordering has been reported both for layered $[Fe^{II}(TCNE^{\bullet-})(NCMe)_2][Fe^{III}Cl_4]$, where powder X-ray diffraction suggested a μ_4-$TCNE^{\bullet-}$ ligand bridging four Fe^{II} centers,[15b] and for cross-linked layered $[Fe(TCNE)_2]\cdot zCH_2Cl_2$.[15c] Such studies and the ones generally dealing with μ_4-$TCNX^{n-}$ ligands may provide useful information with respect to magnetic materials.[2,3]

In this work we present results for the complex ions $\{(\mu_4\text{-TCNX})[Fe(CO)_2(C_5H_5)]_4\}^{4+}$ with the frequently used $[Fe(CO)_2(C_5H_5)]^+ = Fp^+$,[16] commercially available for organic synthesis[17] as the tetrafluoroborate. We have recently described the formation of the TCNE compound $\{(\mu_4\text{-TCNE})[Fe(CO)_2(C_5H_5)]_4\}^{4+}$ and showed the unique EPR spectrum of its one-electron reduced form, exhibiting carbonyl ^{13}C and ^{57}Fe isotope hyperfine coupling.[18] Herein we present DFT calculation results of the geometrical and electronic structure of the compounds $\{(\mu_4\text{-TCNE})[Fe(CO)_2(C_5H_5)]_4\}^{4+/3+}$ and describe the analogues $\{(\mu_4\text{-TCNQ})[Fe(CO)_2(C_5H_5)]_4\}^{4+/3+}$ and $\{(\mu_4\text{-TCNB})[Fe(CO)_2(C_5H_5)]_4\}^{4+}$. The results are put in perspective in comparison to related compounds $(\mu_4\text{-TCNX})[ML_n]_4$.

Experimental Section

Instrumentation. EPR spectra were recorded in the X band on a Bruker System ESP 300 equipped with a Bruker ER035M gaussmeter and a HP 5350B microwave counter. Spectra at high frequency (95, 190, 285 GHz) were taken on a laboratory-made spectrometer[19] at the Grenoble High Magnetic Field Laboratory in frozen solutions at 5 K. Infrared spectra were obtained using a Perkin-Elmer Paragon 1000 PC FTIR spectrometer. UV−vis absorption spectra were recorded on a Shimadzu UV 3101 PC UV−vis−NIR scanning spectrophotometer. Electrical conductivity in solution was determined using a Systronic 305 conductivity bridge. Cyclic voltammetry was carried out at 100 mV/s scan rate in acetonitrile/0.1 M Bu_4NPF_6 using a three-electrode configuration (glassy carbon electrode, Pt counter electrode, Ag/AgCl reference) and a PAR 273 potentiostat and function generator. UV−vis−NIR and spectroelectrochemical measurements were performed under

(2) (a) Miller, J. S.; Epstein, A. J. *Angew. Chem.* **1994**, *106*, 399; *Angew. Chem., Int. Ed. Engl.* **1994**, *33*, 385. (b) Miller, J. S. *Interface* **2002**, *11*, 22. (c) Yee, G. T.; Manriquez, J. M.; Dixon, D. A.; McLean, R. S.; Groski, D. M.; Flippen, R. B.; Narayan, K. S.; Epstein, A. J.; Miller, J. S. *Adv. Mater.* **1991**, *3*, 30. (d) Manriquez, J. M.; Yee, G. T.; McLean, R. S.; Epstein, A. J.; Miller, J. S. *Science* **1991**, *252*, 1415. (e) Pokhodnya, K. I.; Epstein, A. J.; Miller, J. S. *Adv. Mater.* **2000**, *12*, 410. (f) Wang, G.; Zhu, H.; Fan, J.; Siebodnick, C.; Yee, G. T. *Inorg. Chem.* **2006**, *45*, 1406.

(3) (a) Taliaferro, M. L.; Thorum, M. S.; Miller, J. S. *Angew. Chem.* **2006**, *118*, 5452; *Angew. Chem., Int. Ed.* **2006**, *45*, 5326. (b) Vickers, E. B.; Selby, T. D.; Thorum, M. S.; Taliaferro, M. L.; Miller, J. S. *Inorg. Chem.* **2004**, *43*, 6414. (c) Clérac, R.; O'Kane, S.; Cowen, J.; Ouyang, X.; Heintz, R.; Zhao, H.; Bazile, M. J., Jr.; Dunbar, K. R. *Chem. Mater.* **2003**, *15*, 1840. (d) Miyasaka, H.; Izawa, T.; Takahashi, N.; Yamashita, M.; Dunbar, K. R. *J. Am. Chem. Soc.* **2006**, *128*, 11358.

(4) (a) Skotheim, T. A., Elsenbaumer, R. L., Reynolds, J. R., Eds. *Handbook of Conducting Polymers*, 2nd ed.; Marcel Dekker: New York, 1998. (b) Ishiguro, T.; Yamaji, K.; Sato, G. *Organic Superconductors*; Springer: New York, 1998. (c) Potember, R. S.; Poehler, T. O.; Cowan, D. O. *Appl. Phys. Lett.* **1979**, *34*, 405.

(5) Braun-Sand, S. B.; Wiest, O. *J. Phys. Chem. A* **2003**, *107*, 285.

(6) Hartmann, H.; Sarkar, B.; Kaim, W.; Fiedler, J. *J. Organomet. Chem.* **2003**, *687*, 100.

(7) Baumann, F.; Heilmann, M.; Matheis, W.; Schulz, A.; Kaim, W.; Jordanov, J. *Inorg. Chim. Acta* **1996**, *251*, 239.

(8) Olbrich-Deussner, B.; Kaim, W.; Gross-Lannert, R. *Inorg. Chem.* **1989**, *28*, 3113.

(9) (a) Gross, R.; Kaim, W. *Angew. Chem.* **1987**, *99*, 257; *Angew. Chem., Int. Ed. Engl.* **1987**, *26*, 251. (b) Gross-Lannert, R.; Kaim, W.; Olbrich-Deussner, B. *Inorg. Chem.* **1990**, *29*, 5046.

(10) (a) Hartmann, H.; Kaim, W.; Hartenbach, I.; Schleid, T.; Wanner, M.; Fiedler, J. *Angew. Chem.* **2001**, *113*, 2927; *Angew. Chem., Int. Ed.* **2001**, *40*, 2842. (b) Hartmann, H.; Kaim, W.; Wanner, M.; Klein, A.; Frantz, S.; Duboc-Toia, C.; Fiedler, J.; Zalis, S. *Inorg. Chem.* **2003**, *42*, 7018. (c) See also: Leirer, M.; Knör, G.; Vogler, A. *Inorg. Chem. Commun.* **1999**, *2*, 110.

(11) (a) Moscherosch, M.; Waldhör, E.; Binder, H.; Kaim, W.; Fiedler, J. *Inorg. Chem.* **1995**, *34*, 4326. (b) Waldhör, E.; Kaim, W.; Lawson, M.; Jordanov, J. *Inorg. Chem.* **1997**, *36*, 3248. (c) Záliš, S.; Kaim, W.; Sarkar, B.; Duboc, C. Unpublished results.

(12) Baumann, F.; Kaim, W.; Olabe, J. A.; Parisse, A.; Jordanov, J. *J. Chem. Soc., Dalton Trans.* **1997**, 4455.

(13) Berger, S.; Hartmann, H.; Wanner, M.; Fiedler, J.; Kaim, W. *Inorg. Chim. Acta* **2001**, *314*, 22.

(14) Coordination polymers of μ_4-TCNQ: (a) Shields, L. *J. Chem. Soc., Farady Trans. 2* **1985**, *81*, 1. (b) O'Kane, S. A.; Clérac, R.; Zhao, H.; Ouyang, X.; Galán-Mascarós, J. R.; Heintz, R.; Dunbar, K. R. *J. Solid State Chem.* **2000**, *152*, 159. (c) Campana, C.; Dunbar, K. R.; Ouyang, X. *Chem. Commun.* **1996**, 2427. (d) Miyasaka, H.; Campos-Fernández, C. S.; Clérac, R.; Dunbar, K. R. *Angew. Chem.* **2000**, *112*, 3989; *Angew. Chem., Int. Ed.* **2000**, *39*, 3831. (e) Heintz, R. A.; Zhao, H.; Ouyang, X.; Grandinetti, G.; Cowen, J.; Dunbar, K. R. *Inorg. Chem.* **1999**, *38*, 144. (f) Cotton, F. A.; Kim, Y. *J. Am. Chem. Soc.* **1993**, *115*, 8511.

(15) (a) Diaz, C.; Arancibia, A. *Polyhedron* **2000**, *19*, 137. (b) Pokhodnya, K. I.; Bonner, M.; Her, J.-H.; Stephens, P. W.; Miller, J. S. *J. Am. Chem. Soc.* **2006**, *128*, 15592. (c) Her, J.-H.; Stephens, P. W.; Pokhodnya, K. I.; Bonner, M.; Miller, J. S. *Angew. Chem.* **2007**, *119*, 1543; *Angew. Chem., Int. Ed.* **2007**, *46*, 1521.

(16) (a) Sponsler, M. B. *Organometallics* **1995**, *14*, 1920. (b) Watson, L. A.; Franzman, B.; Bollinger, J. C.; Caulton, K. G. *New J. Chem.* **2003**, *27*, 1769. (c) Dulich, F.; Müller, K.-H.; Ofial, A. R.; Mayr, H. *Helv. Chim. Acta* **2005**, *88*, 1754.

(17) Redlich, M. D.; Mayer, M. F.; Hossain, M. M. *Aldrichim. Acta* **2003**, *36*, 3.

(18) Maity, A. N.; Schwederski, B.; Kaim, W. *Inorg. Chem. Commun.* **2005**, *8*, 600.

(19) Barra, A.-L.; Brunel, L.-C.; Robert, J.-B. *Chem. Phys. Lett.* **1990**, *165*, 107.

argon atmosphere using an optically transparent thin layer electrochemical (OTTLE) cell.[20] The windows of the cell consist of CaF_2 plates. Between the plates there is a spacer into which the working (platinum mesh), auxiliary (platinum mesh), and reference (silver wire as pseudo-reference) electrodes are melt-sealed. ^{57}Fe Mössbauer spectra have been recorded using a conventional spectrometer equipped with a helium cryostat for variable temperatures down to ca. 4 K. The isomer shift values in Table 4 are relative to α-iron. For the source, ^{57}Co in rhodium was used. The data were evaluated using the Recoil (1.03a) Mössbauer analysis program.[21]

Synthesis: General Considerations. Cyclopentadienyldicarbonyl(tetrahydrofuran)iron(II) tetrafluoroborate, tetracyanoethene (TCNE), and 7,7,8,8-tetracyano-*p*-quinodimethane (TCNQ) were obtained from Aldrich and Merck, respectively. 1,2,4,5-Tetracyanobenzene (TCNB) was purchased from Fluka. All reactions were carried out under argon using standard Schlenk techniques; the sensitivity of the tetranuclear complexes toward ambient light necessitated the use of tinted glassware. The synthesis of $\{(\mu_4\text{-TCNE})[Fe(CO)_2(C_5H_5)]_4\}(BF_4)_4$ (**1**$(BF_4)_4$) was reported earlier.[18] Its conductivity was measured at 490 Ω^{-1} cm^2 mol^{-1} in CH_3CN (480 Ω^{-1} cm^2 mol^{-1} calculated for a 1:4 electrolyte). The infrared spectrum taken in KBr exhibits bands at ν(CN) = 2269, 2238 cm^{-1} and ν(CO) = 2073, 2027 cm^{-1}.

Synthesis of $\{(\mu_4\text{-TCNQ})[Fe(CO)_2(C_5H_5)]_4\}(BF_4)_4$ ($2(BF_4)_4$). Amounts of 0.016 g (0.08 mmol) of TCNQ and of 0.108 g (0.32 mmol) of $[Fe(CO)_2(C_5H_5)(THF)](BF_4)$ were dissolved in 10 and 20 mL of degassed CH_2Cl_2, respectively. The TCNQ solution was added dropwise to the stirred solution of $[Fe(CO)_2(C_5H_5)(THF)](BF_4)$. Subsequent stirring of the mixture for 20 h in the absence of light produced a blue precipitate. After filtration by canula and washing with CH_2Cl_2, $\{(\mu_4\text{-TCNQ})[Fe(CO)_2(C_5H_5)]_4\}(BF_4)_4$ was obtained as a blue solid at 68.9% yield (0.092 g, 0.078 mmol). Anal. Calcd for $C_{40}H_{24}B_4F_{16}Fe_4N_4O_8$: C, 38.15; H, 1.92; N, 4.45. Found C, 37.61; H, 2.04; N, 4.42. IR (KBr) [ν_{str} (cm^{-1})]: 2255 w (CN), 2236 m (CN), 2180 w (CN), 2074 vs (CO), 2032 vs (CO). Traces of the paramagnetic trication precluded ^{1}H NMR measurements.

Synthesis of $\{(\mu_4\text{-TCNB})[Fe(CO)_2(C_5H_5)]_4\}(BF_4)_4$ ($3(BF_4)_4$). Amounts of 0.009 g (0.05 mmol) of TCNB and of 0.075 g (0.22 mmol) of $[Fe(CO)_2(C_5H_5)(THF)](BF_4)$ were dissolved in 10 mL of degassed CH_2Cl_2 each. The TCNB solution was added dropwise to the stirred solution of $[Fe(CO)_2(C_5H_5)(THF)](BF_4)$. Subsequent stirring of the mixture for 20 h in the absence of light produced a dark yellow precipitate. After filtration by canula and washing with CH_2Cl_2, $\{(\mu_4\text{-TCNB})[Fe(CO)_2(C_5H_5)]_4\}(BF_4)_4$ was obtained as a dark yellow solid at 69.3% yield (0.092 g, 0.078 mmol). Anal. Calcd for $C_{38}H_{22}B_4F_{16}Fe_4N_4O_8$: C, 37.01; H, 1.80; N, 4.54. Found C, 36.55; H, 1.81; N, 4.51. IR (KBr) [ν_{str} (cm^{-1})]: 2285 m (CN), 2075 vs (CO), 2034 vs (CO). ^{1}H NMR (CD_3CN): δ 5.44 (s, broad, 20 H, C_5H_5), 8.59 (s, broad, 2H, TCNB protons).

Quantum Chemical Calculations. The electronic structures of the complexes $\{(\mu\text{-TCNX})[Fe(CO)_2(C_5H_5)]_4\}^{n+}$ and of the TCNX ligands, TCNX = TCNE and TCNQ, were calculated by density functional theory (DFT) methods using the ADF2006.01[22] and Turbomole V5.9[23] program packages. Slater type orbital (STO) basis sets of triple-ζ quality with two polarization functions for Fe and for N, C, and O atoms within the TCNX and CO ligands and of double-ζ quality with polarization functions for the remaining atoms were employed. During the geometry optimization the inner shells were represented by the frozen core approximation (1s for C, N, and O and 1s−3p for Fe were frozen). The core electrons were included in the calculations of **A** tensors. The density functional with local density approximation (LDA) and VWN parametrization of electron gas data including Becke's gradient correction[24a] to the local exchange expression in conjunction with Perdew's gradient correction[24b] to the LDA correlation was used (ADF/BP). The scalar relativistic (SR) zero-order regular approximation (ZORA) was used within ADF calculations of EPR parameters.[25a] The **g** tensor was obtained from a spin-nonpolarized wave function after incorporating the spin−orbit (SO) coupling, and **A** tensors were calculated by an unrestricted approach. **A** tensors and the **g** tensor were obtained by first-order perturbation theory from the ZORA Hamiltonian in the presence of a time-independent magnetic field.[25b,c]

Within Turbomole, a triple-ζ basis with polarization functions for Fe and a double-ζ basis for the remaining atoms[26a] together with the hybrid functional of Burke, Perdew, and Ernzerhof[26b] were used. Spin densities and charge redistributions were calculated by natural bond orbital analysis incorporated in Turbomole.[26c]

Results and Discussion

Synthesis, Electrochemistry, and UV−Vis−NIR Spectroscopic Characterization. The compounds $\{(\mu_4\text{-TCNX})[Fe(CO)_2(C_5H_5)]_4\}(BF_4)_4$ were obtained in a straightforward way from the reaction of TCNX and solutions of $[Fe(CO)_2(C_5H_5)(THF)](BF_4)$[17] in CH_2Cl_2. The compounds are light sensitive as solids and in solution which affected some of the measurements and precluded single-crystal formation so far; light sensitivity has been noted for related manganese compounds and was attributed to dissociative ligand-field excited states.[27] If reducing impurities are not rigorously excluded, the TCNE and TCNQ complexes contain traces of the one-electron-reduced form $\{(\mu_4\text{-TCNX})[Fe(CO)_2(C_5H_5)]_4\}^{3+}$ as evident from Mössbauer and EPR spectroscopy (cf. below). The reason for this particular sensitivity lies in the unusually positive reduction potentials for the $\{(\mu_4\text{-TCNX})[Fe(CO)_2(C_5H_5)]_4\}^{4+/3+}$ couples as reported earlier for the TCNE system (E = +0.48 V vs $Fc^{+/o}$)[18] and as evident from Table 1.

The reduction of the complex ions $\{(\mu_4\text{-TCNX})[Fe(CO)_2(C_5H_5)]_4\}^{4+}$ occurs in two reversible steps for TCNX = TCNE or TCNQ (Figure 1) with typically diminished potential differences (Table 1) as resulting from the ac-

(20) Krejèik, M.; Danek, M.; Hartl, F. *J. Electroanal. Chem.* **1991**, *317*, 179.

(21) Rancourt, D. G.; Lagarec, K. *Nucl. Instrum. Methods Phys. Res.* **1997**, *B129*, 266.

(22) (a) Fonseca Guerra, C.; Snijders, J. G.; Te Velde, G.; Baerends, E. J. *Theor. Chem. Acc.* **1998**, *99*, 391. (b) te Velde, G.; Bickelhaupt, F. M.; van Gisbergen, S. J. A.; Fonseca Guerra, C.; Baerends, E. J.; Snijders, J. G.; Ziegler, T. *J. Comput. Chem.* **2001**, *22*, 931. (c) *ADF2006.01, SCM*; Theoretical Chemistry, Vrije Universiteit: Amsterdam, The Netherlands, 2006; http://www.scm.com.

(23) Ahlrichs, R.; Bär, M.; Häser, M.; Horn, H.; Kölmel, C. *Chem. Phys. Lett.* **1989**, *162*, 165.

(24) (a) Becke, A. D. *Phys. Rev. A* **1988**, *38*, 3098. (b) Perdew, J. P. *Phys. Rev. B* **1986**, *33*, 8822.

(25) (a) van Lenthe, E.; Ehlers, A. E.; Baerends, E. J. *J. Chem. Phys.* **1999**, *110*, 8943. (b) van Lenthe, E.; van der Avoird, A.; Wormer, P. E. S. *J. Chem. Phys.* **1998**, *108*, 4783. (c) van Lenthe, E.; van der Avoird, A.; Wormer, P. E. S. *J. Chem. Phys.* **1997**, *107*, 2488.

(26) (a) Weigend, F.; Ahlrichs, R. *Phys. Chem. Chem. Phys.* **2005**, *7*, 3297. (b) Perdew, J. P.; Ernzerhof, M.; Burke, K. *J. Chem. Phys.* **1996**, *105*, 9982. (c) Reed, A. E.; Weinstock, R. B.; Weinhold, F. *J. Chem. Phys.* **1985**, *83*, 735.

(27) Kaim, W.; Roth, T.; Olbrich-Deussner, B.; Gross-Lannert, R.; Jordanov, J.; Roth, E. K. H. *J. Am. Chem. Soc.* **1992**, *114*, 5693.

Table 1. Reduction Potentials[a] of Complexes $[(\mu_4\text{-TCNQ})(ML_n)_4]$ from Cyclic Voltammetry

ML_n	$E_{1/2}$(red1)	$E_{1/2}$(red2)	solvent/0.1 M Bu_4NPF_6	ref
$[Re(CO)_3(bpy)]^+$	+0.45	+0.09	CH_2Cl_2	10
$[Fe(CO)_2(C_5H_5)]^+$	+0.31	+0.01	CH_3CN	this work
$Os(CO)(P^iPr)_2(H)Cl$	−0.20	−0.94	CH_2Cl_2	12
	−0.25	−0.97	CH_3CN	1a
$Mn(CO)_2(C_5Me_5)$	−0.58	−0.80	DMF[b]	9
$[Ru(NH_3)_5]^{2+}$	−0.59	−0.84	CH_3CN	11a
$[Fe(dppe)(C_5H_5)]^+$	−1.11	−1.26	CH_2Cl_2[b]	15a

[a] In V vs ferrocenium/ferrocene. [b] Recalculated from the SCE reference value.

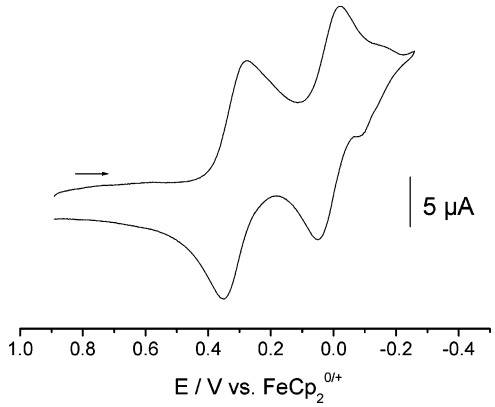

Figure 1. Cyclic voltammogram of $\{(\mu_4\text{-TCNQ})[Fe(CO)_2(C_5H_5)]_4\}(BF_4)_4$ in CH_3CN/0.1 M Bu_4NPF_6 (scan rate: 100 mV/s).

cumulated positive charge in the complexes. The TCNB analogue exhibits only a cathodic peak signal for irreversible reduction.

Vibrational frequencies and absorption maxima for the complex ions $\{(\mu_4\text{-TCNX})[Fe(CO)_2(C_5H_5)]_4\}^{4+}$ are listed and compared in the Experimental Section and in Tables 2 and 3.[18] The characteristic nitrile stretching frequencies ν(CN) have proven to be very valuable indicators of the structural and charge situation of coordinated TCNX.[1] The TCNE and TCNQ complexes exhibit two bands in their infrared spectra in agreement with the ligand symmetry D_{2h} (IR-active modes B_{2u} and B_{3u}). In the case of the TCNB compound, the bands are overlapping and only one band maximum could be determined. This observation may reflect the fact that the symmetry of the TCNB ligand deviates less from D_{4h} (corresponding approximately to a square structure) for which only one band would be expected in the IR spectrum (degenerated E_u mode).

Tables 1−3 and the data from ref 18 illustrate that the complex tetracations $\{(\mu_4\text{-TCNX})[Fe(CO)_2(C_5H_5)]_4\}^{4+}$ are *more easily* reduced and exhibit nitrile stretching bands shifted to *higher* energy relative to those of the free ligands. In addition, the long-wavelength absorption appears at comparatively high energies, a behavior which has previously been observed only for the structurally characterized $\{(\mu_4\text{-TCNQ})[Re(CO)_3(bpy)]_4\}^{4+}$ ion.[10a,b] In all other instances,[6−9,11−13] the π back-donation from the metals into the already low-lying π^* MO of the TCNX bridging ligand causes a cathodic potential shift for the reduction and a low-energy shift of ν(CN) (Tables 1−3).[18] In those cases the fourfold π back-donation appears to stabilize the tetranuclear complexes even in the absence of chelate effects.

Mössbauer Spectroscopy. The lack of π back-bonding in the present case is also evident from Mössbauer spectroscopy (Figure 2) of $\{(\mu_4\text{-TCNX})[Fe(CO)_2(C_5H_5)]_4\}(BF_4)_4$, TCNX = TCNE and TCNQ, which reveals a low-spin iron(II) situation for the main component at 85 and 240/260 K, the parameters only marginally shifted in relation to those of the precursor $[Fe(CO)_2(C_5H_5)(THF)](BF_4)$. This observation supports the notion of absent electron transfer in the ground state. Air- and light-sensitivity of the precursor and of the products result in the formation of high-spin Fe^{II} and Fe^{III} impurities, possibly via dissociation.

^{57}Fe Mössbauer spectra have been recorded of the two compounds under study, $[(\mu_4\text{-TCNE})Fp_4](BF_4)_4$ and $[(\mu_4\text{-TCNQ})Fp_4](BF_4)_4$, where $Fp^+ = [Fe(CO)_2(C_5H_5)]^+$, and, for comparison, the reference compound $[Fp(THF)](BF_4)$. The reference sample and the TCNE complex were measured at 260 and 85 K. The TCNQ derivative was measured at 240 and 85 K. The spectra are displayed in Figure 2. The 260 K spectrum of the reference compound showed three different resonance signals. The dominating one with area fraction 67% is a quadrupole doublet with 0.21 mm s^{-1} isomer shift and 1.93 mm s^{-1} quadrupole splitting. The latter is a consequence of the strong deviation from regular octahedral symmetry, causing anisotropic covalency. The quadrupole splitting determined at 85 K is 1.95 mm s^{-1} and thus within the error limits temperature independent. These parameter values are characteristic of iron(II) in the low-spin state. This assignment is supported by the fact that the quadrupole splitting is indeed temperature independent; the splitting derived from the spectrum recorded at 85 K is 1.95 mm s^{-1}, thus within the error limits the same as that at 260 K. The considerable change of the area fraction from 67% at 260 K to 85% at 85 K looks surprising at first glance; this is a result of the different temperature behavior of the Mössbauer−

Table 2. Vibrational Data and Absorption Maxima λ_{max} of Tetranuclear Complexes $[(\mu_4\text{-TCNQ})(ML_n)_4]$

ML_n	$\tilde{\nu}_{CN}$ (cm^{-1})	$\tilde{\nu}_{CO}$ (cm^{-1})	λ_{max} (nm)	ref
$[Fe(CO)_2(C_5H_5)]^+$	2255 sh, 2236 m	2074 vs, 2032 vs	602/CH_3CN[a]	this work
$[Re(CO)_3(bpy)]^+$	2235 w	2050, 1970	680/CH_2Cl_2	10a,b
	2228			13
$Re(CO)_4Cl$	2245, 2140	1935, 1885	660/C_7H_8	10c
$Cu(Me_3TACN)]^+$	2213 s, 2158 s		*b*	13
$Os(CO)(P^iPr_3)_2(H)Cl$	2180 s, 2140 s	1930 s, 1905 vs	1170/DCE	12
$Mn(CO)_2(C_5Me_5)$	2170 w, 2105 s	1950 w, 19890 vs	1418/C_7H_8	9
$[Ru(NH_3)_5]^{2+}$	2155 s, 2099 vs		935/CH_3CN	11a
$[Fe(dppe)(C_5H_5)]^+$	2099, 2032		1008/CH_2Cl_2	15a

[a] ϵ = 46 600 M^{-1} cm^{-1}. Further absorption at λ_{max} = 364 nm, ϵ = 27 100 M^{-1} cm^{-1}. [b] Insoluble.

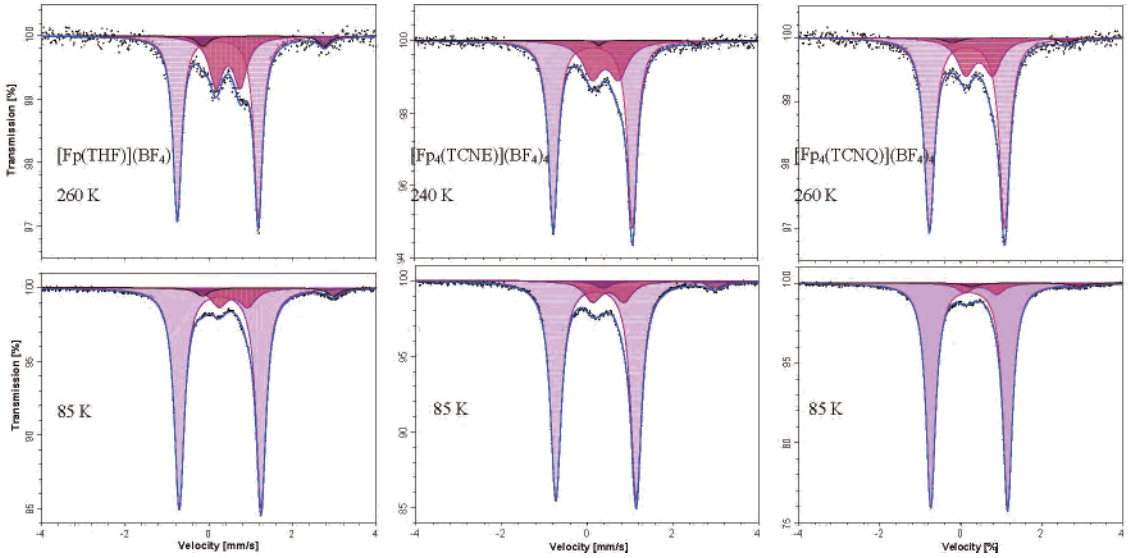

Figure 2. Mössbauer spectra of the reference compound [Fp(THF)]BF_4 at 260 and 85 K, of {(μ_4-TCNE)[$Fe(CO)_2(C_5H_5)]_4$}$(BF_4)_4$ at 240 and 85 K, and of {(μ_4-TCNQ)[$Fe(CO)_2(C_5H_5)]_4$}$(BF_4)_4$ at 260 and 85 K.

Table 3. Vibrational Data, Reduction Potentials, and Absorption Maxima of Tetranuclear Complexes [(μ_4-TCNB)$(ML_n)_4$]

ML_n	$\tilde{\nu}_{CN}$ (cm^{-1})[a]	$E_{1/2}$(red)[b]	λ_{max} (nm)[c]	ref
$[Fe(CO)_2(C_5H_5)]^+$	2285 m[d]	−1.04[e]	400, 323	this work
	2245	−1.06		13
$[Cu(Me_3TACN)]^+$	2212[f]	−1.05	549, 372[g]	13
$Os(CO)(P^iPr_3)(H)Cl$	2185	−1.10[h]	673, 471[g]	12
$[Ru(NH_3)_5]^{2+}$	2164	−0.66	554, 420	11a

[a] In KBr, except where noted. [b] In CH_3CN/0.1 M Bu_4NPF_6, except where noted. Potentials in V vs ferrocenium/ferrocene. [c] In CH_3CN, except where noted. [d] $\tilde{\nu}_{CO}$ = 2075 vs, 2034 vs, 2000 sh (cm^{-1}). [e] Cathodic peak potential for irreversible reduction. [f] In nujol. [g] In 1,2-dichloroethane. [h] In CH_2Cl_2/0.1 M Bu_4NPF_6.

Lamb factor which reflects, with decreasing temperature, a higher relative amount of the iron(II) low-spin component due to its stronger metal−ligand bonds as compared to the high-spin components. The quadrupole doublet with 28% area fraction, 0.48 mm s^{-1} isomer shift, and 0.58 mm s^{-1} quadrupole splitting is characteristic for iron(III) in the high-spin state. In this case the five d orbitals are singly occupied and there is no electric field gradient contribution expected irrespective of any distortion of the local symmetry. The small quadrupole splitting originates from anisotropic covalency (often referred to as *lattice contribution to the field gradient*) caused by the noncubic local symmetry. The weakest quadrupole doublet with ca. 5% area fraction, 1.31 mm s^{-1} isomer shift, and 2.90 mm s^{-1} quadrupole splitting refers unambiguously to iron(II) in the high-spin state. Typical in this case is the relatively large quadrupole splitting, which is mainly caused by the noncubic electronic population of the molecular orbitals around the metal center giving rise to a nonzero electric field gradient. The observed quadrupole splitting in fact increases from 2.90 mm s^{-1} at 260 K to 3.12 mm s^{-1} at 85 K which is typical for iron(II) in the high-spin state.

The Mössbauer spectra of the two samples under study, the TCNE and TCNQ derivatives (Figure 2), do not differ significantly from one another and resemble very much those of the reference samples.[28] The spectra of {(μ_4-TCNE)[$Fe(CO)_2(C_5H_5)]_4$}$(BF_4)_4$ recorded at 260 K (top) and at 85 K (bottom) are shown in Figure 2. They also consist of the three components as discussed above in the case of the reference compound, which even have very similar parameter values as can be seen from Table 4. This clearly indicates negligible metal-to-ligand electron transfer in the ground state, corresponding to a largely unperturbed $(TCNX^\circ)(Fe^{II})_4$ formulation of oxidation states.

These results may seem unsurprising because the $[Fe(CO)_2(C_5R_5)]^+$ cations are not normally considered strong electron donors or acceptors. However, there has been a report where alkyl substitution in the cyclopentadienide ring caused the high persistence of a correspondingly reduced neutral ferrocenyl species $[Fe(CO)_2(C_5R_5)]^\bullet$, R = isopropyl.[29] The EPR data $g_\perp = 2.1215$ and $g_\parallel = 2.1534$ indicated significant metal contribution to the SOMO in this Fe^I species, a result very different from that observed for the ions {(μ_4-TCNX)-$[Fe(CO)_2(C_5H_5)]_4$}$^{3+}$ which involve anion radical ligands (cf. below).

DFT Calculations of Structures. The formulation derived experimentally as {(μ_4-$TCNX^o$)$[Fe^{II}(CO)_2(C_5H_5)]_4$}$^{4+}$ is confirmed by DFT calculations for the TCNE and TCNQ complexes, yielding essentially planar energy minimum structures for the bridging ligands, as appropriate for unreduced TCNE and TCNQ.[1,14,30] Both methods indicate that the most stable configuration of the quadruply charged systems is the closed-shell singlet state involving unreduced TCNX° bridging ligands. During the reduction the doublet

(28) Bermejo, M.-J.; Martínez, B.; Vinaixa, J. *J. Organomet. Chem.* **1986**, *304*, 207.
(29) (a) Sitzmann, H.; Dezember, T.; Kaim, W.; Baumann, F.; Stalke, D.; Kärcher, J.; Dormann, E.; Winter, H.; Wachter, C.; Kelemen, M. *Angew. Chem.* **1996**, *108*, 3013; *Angew. Chem., Int. Ed. Engl.* **1996**, *35*, 2872. (b) Electron transfer from $[(C_5Me_5)Fe(CO)_2]^\bullet$ radicals to TCNE and TCNQ has been inferred from EPR studies: Bergamini, P.; Sostero, S.; Traverso, O. *Inorg. Chim. Acta* **1987**, *134*, 255.
(30) Zhao, H.; Heintz, R. A.; Dunbar, K. R. *J. Am. Chem. Soc.* **1996**, *118*, 12844.

Table 4. ^{57}Fe Mössbauer Data of Complexes ($Fp^+ = [Fe(CO)_2(C_5H_5)]^+$)[a]

complex	T (K)	δ (mm/s)	Δ (mm/s)	$w+$ (mm/s)	populatn (%)
$[Fp(THF)](BF_4)$	85	0.266(1)	1.951(2)	0.144(1)	84.6(6)
		0.58(2)	0.68(3)	0.23(2)	11.3(6)
		1.41(2)	3.12(4)	0.19(3)	4.1(6)
$[(\mu_4\text{-TCNE})Fp_4](BF_4)_4$	85	0.207(1)	1.876(2)	0.153(1)	83.6(6)
		0.50(1)	0.72(2)	0.24(2)	12.0(6)
		1.67(3)	2.63(5)	0.22(4)	4.4(7)
$[(\mu_4\text{-TCNQ})Fp_4](BF_4)_4$	85	0.209(1)	1.901(1)	0.143(1)	92.2(5)
		0.49(2)	0.79(4)	0.21(3)	5.9(6)
		1.60(5)	2.62(9)	0.20(8)	1.9(6)
$[Fp(THF)](BF_4)$	260	0.210(3)	1.934(6)	0.125(5)	67(2)
		0.46(2)	0.58(3)	0.20(5)	28(2)
		1.31(6)	2.90(2)	0.17(9)	5(3)
$[(\mu_4\text{-TCNE})Fp_4](BF_4)_4$	260	0.153(2)	1.845(4)	0.133(3)	72(2)
		0.45(2)	0.62(3)	0.26(3)	26(2)
		1.44(6)	2.3(1)	0.10(8)	1.5(1.1)
$[(\mu_4\text{-TCNQ})Fp_4](BF_4)_4$	240	0.160(3)	1.863(5)	0.152(4)	74(2)
		0.46(2)	0.67(4)	0.26(3)	23(2)
		1.2(2)	2.8(3)	0.23(17)	3(2)

[a] Main component (low-spin Fe^{II}) in first line, followed by high-spin Fe^{III} and Fe^{II} products (see text).

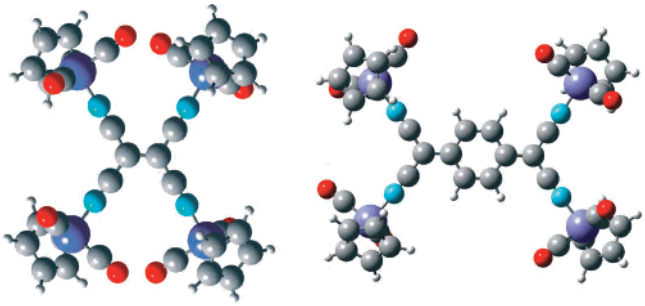

Figure 3. DFT-optimized structures of complexes $\{(\mu_4\text{-TCNX})[(Fe(CO)_2(C_5H_5)_4]\}^{4+}$ (left, TCNE; right, TCNQ).

state with the unpaired electron located in the lowest π^* molecular orbital of the TCNX ligands is being formed.

The optimized structures of the molecular ions $\{(\mu_4\text{-TCNX})[Fe(CO)_2(C_5H_5)]_4\}^{n+}$, TCNX = TCNE or TCNQ, were calculated using DFT methodology without geometrical constraints for the $n = 3$ and $n = 4$ states. The results for the 4+ ions are depicted in Figure 3; the twist between the FeNCCCNFe moieties is less than 10°. The size and low symmetry of the Fp group allow for different conformations resulting from torsion around the Fe−N bonds with the C_5H_5 rings either above or below the approximately planar Fe_4(TCNX) section. The lowest energy conformations involve a *syn* arrangement in the dicyanomethyl sections and an *anti* positioning across the central π systems (Figure 3). For the TCNE complex the calculated Fe−Fe distances are 7.53 Å (1,1 positions), 6.10 Å (*Z*-1,2 positions), and 9.71 Å (*E*-1,2 position, "diagonal"). For the TCNQ analogues, the numbers are 7.23 Å (1,1), 10.83 Å (*Z*-1,2), and 13.03 Å (*E*-1,2). The diminished steric repulsion in the TCNQ analogues has been discussed before for the structurally characterized $[(\mu_4\text{-TCNQ})[Re(CO)_3(bpy)]_4](BF_4)_4$;[10a,b] the TCNE analogue proved to be thermally unstable which was attributed to steric hindrance.[10b] The geometries of other conformers formed by rotation of the $[Fe(CO)_2(C_5H_5)]^+$groups have slightly higher energies; however, the energy differences between the *syn*-1,1 form and, e.g., the *syn*-*Z*-1,2 or *syn*-*E*-1,2 species do not exceed 3 kcal/mol. A list of bond lengths and angles for the complexes and free ligands as optimized by using identical basis sets is given in Tables 5 and 6, showing a slight exaggeration of the calculated central CC bonds (ca. 1.40 Å) relative to experimental structures of TCNE and its complexes (ca. 1.35 Å).[1b] Nevertheless, the comparison of bond parameters of free and coordinated ligands indicates the presence of radical anion ligands within the one-electron-reduced complexes through calcu-

Table 5. Selected DFT-Calculated Averaged Bond Lengths and Angles of Complexes $\{(\mu_4\text{-TCNE})[(Fe(CO)_2(C_5H_5)_4]\}^{n+}$

param	$n = 4$	$n = 3$	TCNE	$TCNE^{\bullet-}$
	Bond Lengths (Å)			
Fe−N	1.864	1.890		
Fe−C(Cp)	2.125	2.110		
Fe−C(CO)	1.794	1.785		
C−N	1.173	1.170	1.164	1.173
C1−C(CN)	1.414	1.401	1.424	1.409
C1−C1′	1.418	1.453	1.379	1.444
	Bond Angles (deg)			
Fe−N−C	177.1	176.3		
N−C−C1	175.5	176.9	179.0	179.1
C−C1−C1′	122.1	122.5	121.3	121.7
C−C1−X	116.7	116.4	117.2	116.7
	Torsional Angles (deg)			
N−C1−C1′−N′	6.0	2.67		
Fe−C1−C1′−Fe′	9.9	7.28		

Table 6. Selected DFT-Calculated Averaged Bond Lengths and Angles of Complexes $\{(\mu_4\text{-TCNQ})[(Fe(CO)_2(C_5H_5)_4]\}^{n+}$

param	$n = 4$	$n = 3$	TCNQ	$TCNQ^{\bullet-}$
	Bond Lengths (Å)			
Fe−N	1.869	1.897		
Fe−C(Cp)	2.124	2.112		
Fe−C(CO)	1.796	1.778		
C−N	1.172	1.170	1.166	1.172
C7−C(CN)	1.410	1.404	1.422	1.411
C1−C7	1.410	1.441	1.401	1.434
C1−C2	1.426	1.420	1.440	1.423
C2−C3	1.368	1.375	1.360	1.376
	Bond Angles (deg)			
Fe−N−C	178.0	176.0		
N−C−C7	175.8	176.9	179.3	176.9
C−C7−C	113.6	113.9	116.7	117.1
C−C7−C1	123.1	123.0	121.6	121.4
	Torsional Angles (deg)			
N−C7−C7′−N′	4.7	2.3		
Fe−C7−C7′−Fe′	8.9	7.3		

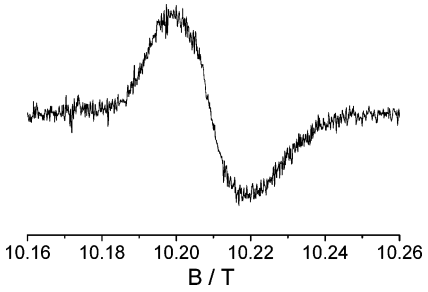

Figure 4. High-frequency (285 GHz) EPR spectrum of $\{(\mu_4\text{-TCNQ})[(Fe(CO)_2(C_5H_5)]_4\}^{3+}$ in CH_2Cl_2/toluene (4/1) at 5 K.

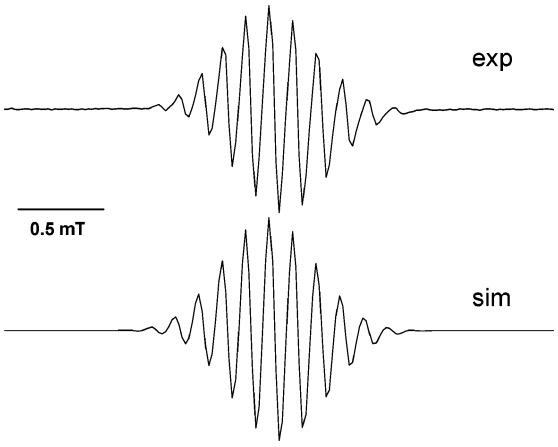

Figure 5. Room-temperature X-band EPR spectrum of $\{(\mu_4\text{-TCNQ})[(Fe(CO)_2(C_5H_5)]_4\}^{3+}$ in CH_2Cl_2 (top) and computer simulation (bottom).

lated (Table 5) and experimentally observed lengthening of that bond by about 0.05 Å.[1b]

EPR Spectroscopy and DFT Calculations. The most compelling evidence for the preferential electron addition in the bridge of complexes $\{(\mu_4\text{-TCNX})[Fe(CO)_2(C_5H_5)]_4\}^{4+}$ comes from EPR spectroscopy of the one-electron-reduced forms. Both species $\{(\mu_4\text{-TCNX})[Fe(CO)_2(C_5H_5)]_4\}^{3+}$ (TCNX = TCNE, TCNQ) exhibit signals at g very close to 2 and without any discernible g anisotropy in frozen solution, even under very high frequency conditions (285 GHz; Figure 4).

Furthermore, at X-band frequency there is hyperfine coupling detectable in fluid solution at room temperature which shows a typical[31,32] increase of the hyperfine constant of the metal-coordinated nitrogen atoms (Figures 5 and 6; Table 5). Whereas the TCNQ complex trication exhibits the ^1H and ^{14}N coupling of coordinating $TCNQ^{\bullet-}$ (Figure 5), the resolved EPR spectrum of $\{(\mu_4\text{-TCNE})[Fe(CO)_2(C_5H_5)]_4\}^{3+}$ does not only reveal coupling from the ^{14}N and ^{13}C nuclei of the TCNE radical ligand but also, after careful analysis, the ^{57}Fe and ^{13}C (CO) hyperfine interaction at the order of about 0.05 mT (Figure 6 and expanded version in Figure S1; Table 7).[18] Thus, the small line width of only 0.01 mT and the small size as well as the high symmetry of the system allowed us to detect the marginal spin transfer from the bridge to the organometallic complex fragments, taking advantage also of the rather covalent metal−carbonyl bond. Within the series of stable transition metal isotopes the

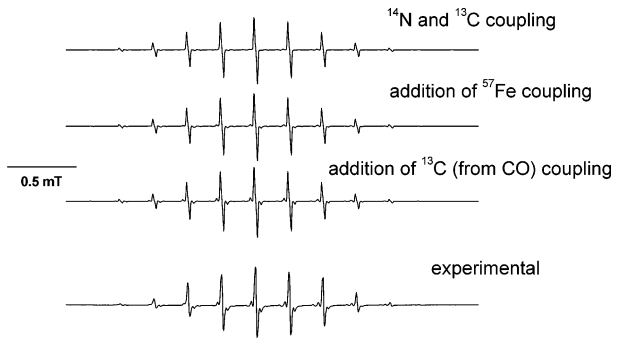

Figure 6. Room-temperature X-band EPR spectrum of $\{(\mu_4\text{-TCNE})[(Fe(CO)_2(C_5H_5)]_4\}^{3+}$ in CH_2Cl_2 (bottom) with various computer-simulated spectra.

^{57}Fe nucleus ($I = 1/2$, 2.15% natural abundance) has the smallest isotropic hyperfine constant a_{iso}[33] which usually precludes observation of corresponding hyperfine structure, even in enriched material.[34] Nevertheless, the ratio of 0.0021 between the observed coupling constant of 0.055 mT to a_{iso} = 26.662 mT[33] is typical for radical anion complexes.[31,32]

ADF/BP86 calculations provide estimates of about 0.168 and 0.128 for the combined spin densities on the metal centers and 0.836 and 0.882 on the TCNX ligands (Table 8) in the TCNE and TCNQ radical complex, respectively. Turbomole calculations using the PBE0 functional show similar spin densities both on the metal centers and the TCNX ligands.

The set of closely lying highest occupied molecular orbitals (HOMOs) of the $\{(\mu_4\text{-TCNX})[Fe(CO)_2(C_5H_5)]_4\}^{4+}$ complexes is formed predominantly by $Fe(CO)_2(C_5H_5)$ fragment orbitals whereas the lowest lying unoccupied orbitals (LUMOs) are formed mainly from the π^* orbitals of the TCNX ligands. Identical sequences of frontier orbitals are obtained if either pure BP86 or hybrid PBE0 functionals were used. The electron added on reduction is taken up by this orbital; the reduction therefore influences mainly the TCNX ligand. Nevertheless, the $[Fe(CO)_2(C_5H_5)]^+$ complex fragments are also affected by this reduction, in agreement with the very small but detectable spin delocalization as shown in Tables 7 and 8. Table 8 summarizes the calculated spin densities for all systems studied. This table shows that natural population analysis (Turbomole) gives values of spin densities comparable with ADF/BP calculated ones. The calculations provide estimates of about 0.16 and 0.09−0.13 for the combined spin densities on the metal centers (Table 8) in the TCNE and TCNQ radical complexes, respectively, representing upper limits for the actual metal participation at the singly occupied molecular orbital (SOMO) which would contribute to the anisotropy and to the deviation of g_{iso} from the free electron value. The remaining bulk of spin density is distributed over the TCNE and TCNQ ligands. A comparison of spin densities illustrates the radical anion

(31) Kaim, W. *Coord. Chem. Rev.* **1987**, *76*, 187.
(32) Bell, S. E.; Field, J. S.; Haines, R. I.; Moscherosch, M.; Matheis, W.; Kaim, W. *Inorg. Chem.* **1992**, *31*, 3269.
(33) Weil, J. A.; Bolton, J. R.; Wertz, J. E. *Electron Paramagnetic Resonance*; Wiley: New York, 1994; p 534.
(34) See for instance: (a) Belousov, Y. A.; Kolosova, T. A. *Polyhedron* **1987**, *6*, 1959. (b) DeRose, V. J.; Telser, J.; Anderson, M. E.; Lindahl, P. A.; Hoffman, B. M. *J. Am. Chem. Soc.* **1998**, *120*, 8767. (c) Kaim, W.; Schwederski, B. In *Magnetic Properties of Free Radicals*; Fischer, H., Ed.; Landolt-Börnstein II/26a, 2006; p 1.

Table 7. Comparison of Experimental and Calculated g Values and Hyperfine Coupling Constants (mT) for $\{(\mu\text{-TCNX})[Fe(CO)_2(C_5H_5)]_4\}^{3+}$ and Free Ligand Radical Anions

	complex, TCNX = TCNE		$TCNE^{\bullet-}$		complex, TCNX = TCNQ		$TCNQ^{\bullet-}$	
param	expt	calcd	expt	calcd	expt	calcd	expt	calcd
g_{11}		2.0034	n.d.	2.0038		2.0033	n.d.	2.0033
g_{22}		1.9987	n.d.	2.0027		1.9990	n.d.	2.0031
g_{33}		1.9958	n.d.	2.0021		1.9972	n.d.	2.0021
g_{iso}	1.9965	1.9993	2.0026	2.0029	1.9677	1.9989	2.0027	2.0028
$A(^{14}N)$	0.246	0.146	0.157	0.083	0.137	0.099	0.099	0.057
$A(^{1}H)$					0.139	−0.127	0.142	0.123
$A(^{57}Fe)$	0.055	−0.049			n.o.	n.d.	*d*	*d*
$A(^{13}C)^a$	0.334	0.378	0.292	0.461	n.o.	n.d.	*d*	*d*
$A(^{13}C)^b$	0.912	−0.692	0.945	−0.774	n.o.	n.d.	*d*	*d*
$A(^{13}C)^c$	0.055	0.053			n.o.	n.d.	*d*	*d*

[a] Ethene C. [b] Cyano C. [c] Carbonyl C. [d] Not discussed because data from the complex could not be obtained (n.o. = not observed; n.d. = not determined).

Table 8. DFT-Calculated Averaged Spin Densities for Complexes $\{(\mu_4\text{-TCNX})[(Fe(CO)_2(C_5H_5)_4]\}^{3+}$ and for TCNX Radical Anions[a]

	complex, TCNX = TCNE		$TCNE^{\bullet-}$		complex, TCNX = TCNQ		$TCNQ^{\bullet-}$	
species	A	B	A	B	A	B	A	B
N	0.118	0.138	0.146	0.160	0.082	0.088	0.104	0.120
H					−0.003	−0.001	−0.002	−0.002
C1	0.234	0.259	0.278	0.284	0.067	0.105	0.050	0.055
C2					0.035	0.029	0.041	0.035
C7					0.184	0.191	0.225	0.230
C(CN)	−0.026	−0.051	−0.035	−0.052	−0.019	−0.033	−0.031	−0.046
Fe	0.042	0.041			0.032	0.023		
C(CO)	−0.003	0.006			−0.001	0.002		
Fe(tot.)	0.168	0.164			0.128	0.092		
TCNX(tot.)	0.836	0.866	1.000	1.000	0.882	0.924	1.000	1.000

[a] A: ADF-calculated values, derived from Mulliken population analysis. B: values derived from NBO analysis (Turbomole).

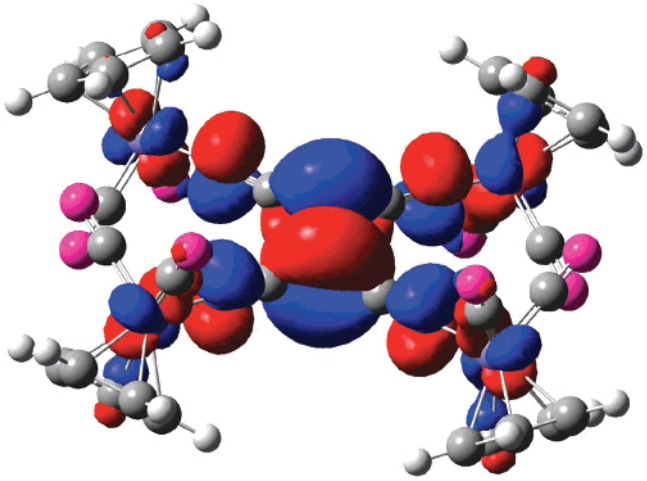

Figure 7. Representation of the LUMO of $\{(\mu_4\text{-TCNE})[(Fe(CO)_2(C_5H_5)]_4\}^{4+}$.

character of the TCNX ligands within the complexes, and the natural population analysis leads to the same conclusion. The LUMO of $\{(\mu_4\text{-TCNE})[Fe(CO)_2(C_5H_5)]_4\}^{3+}$ is depicted in Figure 7.

Calculated g values and hyperfine couplings for the complexes $\{(\mu_4\text{-TCNX})[Fe(CO)_2(C_5H_5)]_4\}^{3+}$, TCNX = TCNE or TCNQ, and of the free ligand radical anions are listed together with the experimental values in Table 7. As shown by Table 8, the DFT calculations confirm the qualitative conclusions on the basis of the population analysis and reproduce the EPR parameters for both complexes quite well. The ^{14}N hyperfine splitting is somewhat underestimated by the calculations, nevertheless, in agreement with the experiment the ^{14}N coupling constants for the radical complexes are larger than those of the free ligand anions.[31,32]

Spectroelectrochemistry. Spectroelectrochemistry of the tetranuclear complexes was affected by their earlier mentioned sensitivity. The TCNE complex in particular turned out to be rather sensitive toward ambient light, a behavior reported similarly for related $Mn(CO)_2(C_5R_5)$ compounds.[27] Due to that low stability and to concentration requirements, spectroelectrochemical studies could only be undertaken in the UV−vis−NIR and IR regions for the reduction of the TCNQ complex (Figure 8). The familiar[10] appearance of the structured NIR bands of the $TCNQ^{\bullet-}$ chromophore was observed in the first reduction step (Figure 8a) and its disappearence in the second step (Figure 8b), confirming the bridging ligand as the main site of electron uptake. The metal carbonyl stretching bands were only slightly influenced, shifted to lower energy by 5−9 cm^{-1} and by 7−10 cm^{-1} in the first and second reduction steps, respectively. Strong absorption by acetonitrile, the only solvent usable for solubility reasons, hindered the observation of the TCNQ nitrile stretching bands via spectroelectrochemistry; C═C vibrations were not clearly detected either.

Irreversibility of even the first reduction of the TCNB[1c] complex at the rather negative potential of about −1 V precluded spectroelectrochemical studies; however, both the high-energy CN stretching frequency at 2285 cm^{-1} and the charge transfer absorptions ≤400 nm (Table 3) also confirm a negligible transfer of electron density from the metal

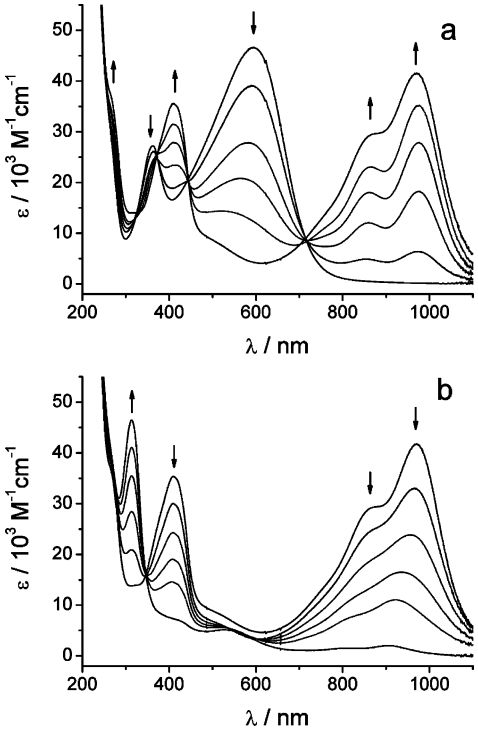

Figure 8. UV−vis−NIR spectroelectrochemistry of $\{(\mu_4\text{-TCNQ})[(Fe(CO)_2(C_5H_5)]_4\}^{4+\rightarrow 3+}$ (a) and $\{(\mu_4\text{-TCNQ})[(Fe(CO)_2(C_5H_5)]_4\}^{3+\rightarrow 2+}$ (b) in CH_2Cl_2/0.1 M Bu_4NPF_6.

complex fragments to the TCNB ligand and the exceptional position of the complexes $\{(\mu_4\text{-TCNX})[Fe(CO)_2(C_5H_5)]_4\}(BF_4)_4$.

Conclusion. Apart from the crystallographically analyzed[10a,b] $\{(\mu_4\text{-TCNQ})[Re(CO)_3(bpy)]_4\}^{4+}$, this is only the second time that discrete tetranuclear complexes of clearly nonreduced electron-deficient TCNX ligands (TCNE, TCNQ) have been characterized. The reluctance of these very strongly "noninnocent" π acceptor ligands to accept electron density from $[Fe(CO)_2(C_5H_5)]^+$ is remarkable, given the capability of neutral manganese analogues $\{(\mu_4\text{-TCNX})[Mn(CO)_2(C_5R_5)]_4\}$ to undergo extensive electron transfer;[9] it can be understood, however, considering the symmetries and very different energies of the available orbitals of the "Fp" group.[16]

Nevertheless, it remains surprising that the extraordinary π acceptors TCNE and TCNQ can still bind up to four non-back-donating first-row transition metal groups in a discrete molecular ion and thus become even easier to reduce than the free ligands. All available experimental and theoretical results confirm the absence of significant π interaction in the nonreduced and reduced (radical anion) states; attempts to further characterize such materials in the corresponding solids will be made.

Taken together with previous results,[9−12,15] the results described here seem to indicate a dichotomy between the systems $\{(\mu_4\text{-TCNQ})[Re(CO)_3(bpy)]_4\}^{4+}$ [10a,b] and the presently described $\{(\mu_4\text{-TCNX})[Fe(CO)_2(C_5H_5)]_4\}^{4+}$, which show no signs of metal-to-TCNX electron transfer as delineated above and as confirmed by calculations, and, on the other side, paramagnetic compounds such as $\{(\mu_4\text{-TCNX})[Ru(NH_3)_5]_4\}^{8+}$,[11] $\{(\mu_4\text{-TCNX})[Mn(CO)_2(C_5R_5)]_4\}$,[9] $\{(\mu_4\text{-TCNX})[Os(H)(Cl)(PR_3)_2(CO)]_4\}$,[12] or $\{(\mu_4\text{-TCNQ})[Fe(C_5H_5)(dppe)]_4\}^{4+}$,[15] which exhibit spectroscopic and electrochemical features of significantly reduced bridging TCNX ligands, i.e., a large δ in the formulation $\{(\mu_4\text{-TCNX}^{\delta-})[M^{x+\delta/4}L_n]_4\}$. This dichotomy between the former $\delta \approx 0$ systems and the latter complexes approaching $\delta \approx 2$ suggests that the intermediate situation with μ_4-$TCNX^{\bullet-}$ and $\delta \approx 1$ may be more difficult to achieve and may require careful orbital energy tuning of the metal components used; however, it possibly constitutes a key to the further development of magnetic materials in this area.[2]

Acknowledgment. Support from the DFG (Priority Program 1137 "Molecular Magnetism"; P.G.) and EU (COST Actions D14 and D35; S.Z. and W.K.) and financial support by the HPC Europa and the Grant Agency of the Academy of Sciences of the Czech Republic (Grant 1ET400400413; S.Z.) is gratefully acknowledged.

Supporting Information Available: Figure S1 of an EPR spectrum. This material is available free of charge via the Internet at http://pubs.acs.org.

IC062253K